

## Effects of operating parameters on time-dependent ash entrainment behaviour of a sample coal flotation

H. Paryad, H. Khoshdast and V. Shojaei\*

*Department of Mining Engineering, Higher Education Complex of Zarand, Zarand, Iran*

Received 11 Novembre 2016; received in revised form 21 January 2017; accepted 28 January 2017

\*Corresponding author: v.shojaei@uk.ac.ir (V. Shojaei).

### Abstract

It is well-known that entrainment of particles into the froth is a key factor in the selectivity and performance of the flotation process, especially for fine particle recovery. Since flotation is a continuous process, in this work, the effects of operating parameters on the entrainment of ash materials in a sample coal flotation is investigated from a time-sequence viewpoint. The effects of the pulp solid content, collector concentration, frother concentration, impeller speed, and particle size on the entrainment factor and water recovery at different flotation times are evaluated using a D-optimal response surface experimental design. The experimental work carried out shows that some parameters, especially particle size and pulp density, can yield completely different responses from those reported in the literature. The observed unusual behaviours can be attributed to the entrainment mechanisms and verified by the experimental results. It is also shown that the dominant entrainment mechanism can be varied by time. In addition, the statistical analyses of the experimental design show that the effects of some parameters change during time from the initial to the final stages of the flotation process. The results obtained indicate that the particle size and pulp density are the most important parameters influencing the entrainment rate and water recovery. The effects of the collector and frother concentrations are less on the entrainment and water recovery. In addition, the interaction between the solid percentage and particle size is the only significant mixed effect.

**Keywords:** *Coal Flotation, Operating Factors, Time Sequence, Entrainment Factor, Water Recovery.*

### 1. Introduction

Froth flotation is a selective process used for separating different minerals from complex ores by utilizing their physico-chemical surface properties [1]. The efficiency and selectivity of the flotation process depend on a large number of factors such as the surface properties and size of the mineral species in the feed material, aeration rate and size of the bubbles, depth of the froth, and rate at which the concentrate is removed. While the efficiency of the process is determined largely by the true flotation of valuable mineral particles that are physically attached to the bubble surfaces, the selectivity is dependent on the degree to which unwanted or gangue particles are entrained with the water occupying the spaces between the bubbles. Hence, in any attempt to model the processes that occur in flotation froths,

it is essential to have reasonable estimates of the contributions made to the flotation process by a true flotation and entrainment [2].

Since entrainment has a detrimental effect on the efficiency of the process, a number of studies have been carried out to understand the entrainment mechanisms and identify the factors affecting entrainment. As reported by Wang et al. [3], the early research work on the characteristics of entrainment was first conducted by Livshits and Bezrodnaya (1961) and Jowett (1966), who studied the factors affecting gangue recovery such as the particle size, pulp density, and amount of water reporting to the concentrate. Such investigations were then followed by a number of authors such as Trahar [4], Warren [5], Kirjavainen [6, 7], Smith and Warren [8], Savassi

et al. [9], Shi and Zheng [10], Akdemir and Sönmez [11], Zheng et al. [12], Yianatos et al. [13], Yianatos and Contreras [14], Konopacka and Drzymala [15], Wiese et al. [16], Kracht et al. [17], Little et al. [18], and Wiese and O'Connor [19], who worked on understanding the factors affecting entrainment from the experimental studies in several flotation systems, with and without floatable minerals, varying the physical characteristics of gangue particles (size, density, and shape) and changing the process variables (e.g. solids percentage, froth depth, and air flow rate). Cilek and Yilmazer [1] and Lima et al. [20] also investigated the effect of hydrodynamic parameters on the entrainment rate.

Although the above-mentioned works give a deep understanding of the entrainment mechanisms and effects of the operating factors and help to develop models with the objective of predicting entrainment in a flotation cell, the following points may challenge the results reported in the literature:

- First, it should be noted that the flotation process is a continuous time-dependent process; whereas all the aforesaid studies have used the equilibrium data to evaluate the entrainment rate of particles, i.e. the data was collected after the flotation process finished and then used to calculate the entrainment factors.

- As reported in almost all papers, the hydraulic entrainment of fine particles in the wake space following the bubbles rising toward the froth phase has been denoted as the main entrainment mechanism and used to interpret the effects of the operating variables on the entrainment behaviour observed in flotation experiments, whereas other mechanisms are also effective.

In the present work, the effects of some important operating parameters on the entrainment response of a sample coal flotation was investigated using the response surface methodology (RSM). The time-dependent entrainment rate of each experiment was calculated and analyzed by statistical approaches to evaluate the main effects of the studied factors as well as their interaction effects.

## 2. Materials and Methods

### 2.1. Coal sample

A representative bituminous coal sample of -500 µm particle size from Zarand Coal Washing Plant (Zarand, Iran) was used in the experimental work. The size distribution of this material is given in Table 1. The mineralogical examinations indicated that the ash material consisted mainly of sheet silicate minerals (> 98%) with some quartz and calcite (< 2%).

**Table 1. Chemical analysis and size distribution of coal sample studied.**

Detailed particle size distribution of feed			Particle size fractions used in this study		
Size (µm)	Retained (wt.%)	Ash content (%)	Size (µm)	Retained (wt.%)	Ash content (%)
+300-500	25.85	28.13	+150-500	53.37	28.05
+150-300	27.52	27.98			
+75-150	16.15	28.57	+45-150	19.03	28.12
+45-75	2.88	25.61			
-45	27.60	39.55	-45	27.60	39.55

### 2.2. Experimental design

Different types of experimental designs are now available. The choice of a suitable design depends on the objectives of the investigation and the number of factors to be investigated. Since the main objective of this work is was expand an appropriate approximating relationship between the flotation responses and the process variables, the response surface methodology (RSM) was selected. RSM is a collection of mathematical and statistical techniques used for empirical model building. In other words, RSM is aimed to model the experimental responses and then migrate into the modelling of numerical experiments. With response surface analysis, we run a series of full factorial experiments and mapped the response to

generate mathematical equations that describe how factors affect the response. Additionally, RSM allows us to estimate the interaction and even quadratic effects, and therefore, gives us an idea of the (local) shape of the response surface we are investigating [21]. The main idea of RSM is to use a set of designed experiments to obtain an optimal response. RSM, involving statistical design of experiments based on the multivariate non-linear model in which all factors are varied over a set of experimental runs, is a combination of mathematical and statistical techniques useful for developing, improving, and optimizing processes and can be used to evaluate the relative significance of some affecting factors even in the presence of complex interactions [22]. Generally,

the following reasons led us to apply RSM in the experimental investigations:

- Due to the orthogonality property of response surface design, individual effects can be estimated independently without (or with minimal) confounding, the problem that is observed in the Taguchi and fractional designs. Also orthogonality provides minimum variance estimates of the model coefficient so that they are uncorrelated.

- RSM uses non-linear functions to model the relationship between the process variables and response(s); therefore, we can find out any possible non-linear effect, either ascent or descent of variables, on process response.

- The property of rotating points of response surface design about the center of the factor space results in the moments of the distribution of the design points becoming constant. Thus the possible errors caused by experimental inadvertences can smoothly be prorated.

In this work, a D-optimal response surface design was applied as an experimental design strategy to investigate the ash entrainment behaviour. D-optimal RSM design is a useful strategy for building a second-order (quadratic) model for the response variables without the need to use a complete three-level factorial experiment. D-optimal design helps modelling both the numeric and categoric (qualitative) factors. Qualitative factors have only discrete values and no continuous scale; therefore, the presence of these discrete steps drastically increases the number of runs for a normal design [23]. Thus the required runs for a D-optimal design are always lower and do not increase as fast as the classical design with a growing number of factors [24]. It is also useful for estimation of the parameters of regression models with continuous variables [21, 25]. The levels of interest for each factor were selected based on the variation ranges of the input and output variables measured during industrial investigations. Table 2 presents the levels of interest for each factor involved for the evaluation of the entrainment rate and water recovery as the process responses. The final experimental design matrix is shown in Table 3.

### 2.3. Flotation tests and entrainment measurement

Flotation tests were carried out in a Denver D-12 flotation machine with a 2-l cell volume. For each semi-batch test, a requisite amount of bulk coal sample was transferred into the cell and additional

tap water (pH 7±0.2) was added to maintain the required pulp density. The impeller speed of the flotation chamber was set, and the pulp was allowed to condition for 5 min. Then the required volume of diesel oil, as collector, was added to the cell and conditioned for other minutes. The frother (MIBC) was subsequently added, and after conditioning for a minute, the air inlet valve was opened and the froth was collected after 10, 20, 30, 60, and 120 s of flotation. When the final froth sample was collected, the machine was stopped. The froth products and the tailings (the part that remained inside the machine) were dried, weighed, and analyzed. Ash analyses were carried out according to ASTM D 3174-73 Standard, showing that the bulk sample contained 29.04% ash. Before ash analysis, the product was first allowed to settle, decanted, and then dried at 60 °C.

The recoveries of water, ash, and coal were calculated as follow [26]:

$$\text{Recovery (Coal, \%)} = \frac{C(100-c)}{F(100-f)} \times 100 \quad (1)$$

$$\text{Recovery (Ash, \%)} = \frac{Cc}{Ff} \times 100 \quad (2)$$

$$\text{Recovery (Water, \%)} = \frac{W_c}{W_f} \times 100 \quad (3)$$

where  $F$  and  $C$  are the weights of feed and concentrate with  $f$  and  $c$  as their corresponding ash percentages, respectively, and  $W_f$  and  $W_c$  are the weights of water in feed and recovered in concentrate, respectively. The coal recovery data was also fitted to the following first-order kinetics model to determine the flotation rate value [27]:

$$R = R_\infty(1 - \exp(-kt)) \quad (4)$$

where  $R$  is the cumulative recovery,  $R_\infty$  is the maximum achievable recovery, and  $t$  and  $k$  are the time (s) and kinetic constant (1/s) of flotation, respectively.

The degree of entrainment was found out by evaluating the “entrainment factor” according to the method described by Yianatos et al. [13]:

$$EF_i = \frac{R_{\text{ash},t}}{W_t} \times 100 \quad (5)$$

where  $EF_t$  (%/g) is the cumulative entrainment factor after  $t$  s of flotation (according to the time-step froth collection),  $R_{\text{ash},t}$  (%) is the cumulative ash recovery to the concentrate product, and  $W_t$  is the cumulative mass recovery of water (g).

**Table 2. Level of variables considered for entrainment rate evaluation by D-optimal RSM design.**

Coded Symbol	Variables	Units	Type	Actual and Center Points		
				-1	0	+1
A	Solid content	%	Numeric	7	9.5	12
B	Collector concentration	g/t	Numeric	900	1200	1500
C	Frother concentration	g/t	Numeric	25	40	55
D	Impeller speed	rpm	Numeric	1000	1250	1500
E	Feed particle size	µm	Categoric	-45	+45-150	+150-500

**Table 3. Experimental design matrix for D-optimal RSM considered in this study.**

Run	Actual variables				
	A	B	C	D	E
	Solid content	Collector conc.	Frother conc.	Impeller speed	Particle size
1	12	1250	25	1000	-500
2	7	1000	25	1500	-150
3	12	1500	25	1250	-150
4	7	1500	55	1250	-45
5	9.5	1000	25	1500	-150
6	7	1250	55	1000	-500
7	7	1000	55	1500	-150
8	9.5	1250	40	1000	-45
9	9.5	1250	55	1000	-500
10	12	1000	55	1500	-150
11	7	1000	55	1500	-45
12	9.5	1250	25	1000	-500
13	9.5	1250	40	1000	-45
14	12	1500	25	1250	-150
15	7	1500	55	1250	-45
16	7	1500	25	1250	-150
17	7	1000	40	1500	-500
18	7	1500	25	1250	-45
19	7	1250	40	1000	-150
20	7	1500	55	1250	-500
21	12	1500	40	1250	-500
22	12	1000	25	1500	-45
23	7	1500	25	1250	-500
24	12	1000	55	1500	-45
25	12	1250	25	1000	-500
26	12	1500	55	1250	-150
27	7	1000	25	1500	-45
28	12	1000	25	1500	-500
29	7	1500	55	1250	-150
30	12	1000	25	1500	-45
31	12	1500	25	1250	-45
32	12	1500	55	1250	-45
33	7	1000	25	1500	-500
34	12	1500	55	1250	-150
35	12	1250	40	1000	-150

**3. Results and discussion**

**3.1. Analysis of variance (ANOVA)**

The entrainment factor and water recovery at each time-step froth sampling were analyzed as process responses. The experimental results for each run are given in Table 4.

By RSM, a quadratic polynomial equation is first applied to yield a preliminary prediction of the response as a function of independent variables involving their interactions [25, 28]. In general,

the experimental data obtained from the designed experiment is analyzed by the response surface regression procedure using the following quadratic polynomial equation:

$$y = b_0 + \sum b_i x_i + \sum b_{ii} x_i^2 + \sum b_{ij} x_i x_j + \varepsilon \quad (5)$$

where y is the predicted response, b<sub>0</sub> is the constant coefficient, b<sub>i</sub> is the linear coefficients, b<sub>ii</sub> is the quadratic coefficient, b<sub>ij</sub> is the interaction

coefficient,  $x_i$  and  $x_j$  are coded values of the independent process variables, and  $\varepsilon$  is the residual error.

After the initial estimated value for the coefficients was calculated, the RSM model was used to evaluate the influence of the process variables on the response(s). Analysis of variance (ANOVA) was performed to test the significance of the model coefficients and parameters. The values for the coefficients were calculated using the Design-Expert Software v.7.1.5. Then the model had to be manually modified by manipulating the parameters involved based on their significance to yield the highest fitting correlation between the predicted and experimental data. In this work, the 2FI model showed the highest prediction precision, and was used to evaluate the influence of the process variables on the entrainment factors and their corresponding water recovery. The model includes the single and double-interaction

parameters, as given in Table 5. The analysis indicated that involving the triple and quadratic interactions within the model equation decreased the model correlation factors, i.e. R-squared and adjusted R-squared factors, and thus they were transferred to error. In addition, despite the very high  $p$ -value, transferring most of the double-interaction parameters to error significantly decreased the model accuracy; therefore, these parameters were used to develop the RSM 2FI model. Due to the multiplicity of responses,  $p$ -values of the ANOVA results are only listed in Table 5. The significance of each effect was determined using the  $p$ -values. “Prob > F” values less than 0.05 (for 95% confidence interval considered in this work) indicate that the effects are significant [21]. The ANOVA results (Table 5) of the 2FI models suggest that all models are highly significant, as it is evident from the Fisher's F-test values with very low probability values ( $p$  model < 0.0001).

**Table 4. Experimental results for measurement of entrainment factor and water recovery.**

Run	Entrainment factor after $t$ s of flotation					Water recovery after $t$ s of flotation				
	10	20	30	60	120	10	20	30	60	120
1	0.204	0.189	0.186	0.173	0.156	6.106	10.895	13.112	14.740	16.487
2	0.179	0.183	0.165	0.154	0.137	3.751	5.918	8.055	10.108	11.575
3	0.137	0.145	0.143	0.140	0.122	10.737	13.520	16.422	18.915	22.602
4	0.048	0.046	0.046	0.044	0.042	2.613	4.451	6.040	8.957	13.336
5	0.088	0.126	0.119	0.109	0.099	3.337	6.007	8.639	11.631	13.665
6	0.318	0.305	0.281	0.258	0.218	4.169	6.681	8.169	9.197	11.090
7	0.124	0.134	0.132	0.125	0.116	3.418	6.896	8.831	10.719	11.933
8	0.038	0.037	0.036	0.035	0.033	1.896	3.457	4.618	7.589	12.784
9	0.241	0.245	0.226	0.214	0.190	5.104	8.342	11.352	12.551	14.293
10	0.083	0.111	0.129	0.126	0.118	5.623	10.122	13.612	18.529	20.706
11	0.030	0.029	0.028	0.028	0.024	1.311	2.394	3.692	5.652	10.205
12	0.214	0.212	0.213	0.203	0.181	4.498	7.469	9.142	10.522	12.104
13	0.041	0.031	0.030	0.033	0.033	1.901	3.715	5.732	8.763	14.929
14	0.127	0.127	0.123	0.117	0.103	10.553	14.578	17.471	20.183	23.533
15	0.048	0.045	0.045	0.044	0.040	2.875	5.791	7.882	11.929	16.700
16	0.211	0.192	0.173	0.161	0.135	5.353	7.832	9.661	11.389	14.807
17	0.283	0.327	0.316	0.298	0.271	2.634	4.700	6.660	8.498	9.501
18	0.044	0.042	0.043	0.041	0.040	1.964	3.857	5.766	9.985	15.941
19	0.207	0.212	0.199	0.182	0.152	6.272	8.700	10.458	6.272	14.938
20	0.334	0.316	0.282	0.250	0.177	4.333	6.562	8.059	9.462	13.500
21	0.180	0.187	0.177	0.171	0.138	5.149	8.200	10.504	13.112	16.808
22	0.015	0.014	0.013	0.014	0.016	1.580	2.972	4.306	6.545	9.921
23	0.305	0.298	0.262	0.234	0.176	3.692	5.896	7.367	8.615	11.679
24	0.011	0.012	0.011	0.011	0.012	1.440	2.524	3.758	5.689	8.410
25	0.251	0.234	0.232	0.205	0.187	4.333	7.317	10.114	12.989	14.525
26	0.118	0.126	0.122	0.120	0.100	13.037	17.089	19.705	22.677	28.137
27	0.018	0.022	0.024	0.025	0.025	1.184	1.833	2.499	3.667	6.225
28	0.174	0.224	0.229	0.212	0.196	3.494	7.019	10.087	13.090	14.358
29	0.218	0.215	0.199	0.175	0.137	7.688	10.651	12.463	14.886	19.409
30	0.020	0.019	0.018	0.020	0.023	1.413	2.744	4.008	6.058	9.117
31	0.032	0.032	0.031	0.032	0.030	1.550	3.099	4.368	7.124	12.396
32	0.031	0.031	0.032	0.034	0.035	3.371	5.913	8.384	12.251	18.054
33	0.297	0.312	0.305	0.290	0.269	3.511	5.795	7.768	8.687	9.416
34	0.130	0.137	0.141	0.140	0.115	10.215	13.015	15.254	19.780	25.556
35	0.122	0.159	0.167	0.165	0.203	6.145	11.264	14.749	19.130	20.429

**Table 5. ANOVA for response surface model of entrainment factor and water recovery.**

Source	<i>p</i> -value (Prob > F) for entrainment factor after <i>t</i> s of flotation					<i>p</i> -value (Prob > F) for water recovery after <i>t</i> s of flotation				
	10	20	30	60	120	10	20	30	60	120
Model	< 0.0001	< 0.0001	< 0.0001	< 0.0001	< 0.0001	< 0.0001	< 0.0001	< 0.0001	< 0.0001	< 0.0001
Model F value	64.5752	42.9322	40.1780	41.1116	13.4474	17.6591	16.6572	19.9615	13.5960	26.4689
R-Sqrd	0.9936	0.9840	0.9829	0.9833	0.9505	0.9619	0.9597	0.9661	0.9510	0.9742
Adj R-Sqrd	0.9782	0.9610	0.9584	0.9593	0.8798	0.9074	0.9021	0.9177	0.8811	0.9374
Pred R-Sqrd	0.8884	0.9188	0.9159	0.9125	0.6777	0.7364	0.7961	0.8086	0.6167	0.7339
Adeq Precision	25.0920	20.0284	20.1231	20.9049	12.6728	14.6891	14.2650	15.6829	13.7403	20.3955
A-Solid content	< 0.0001	< 0.0001	< 0.0001	0.0002	0.0681	0.0027	0.0004	< 0.0001	< 0.0001	< 0.0001
B-Collector conc.	0.0673	0.2375	0.1972	0.2594	0.5118	0.2461	0.1971	0.0687	0.0880	0.0060
C-Frother conc.	0.4909	0.8695	0.9171	0.8195	0.9839	0.0344	0.0131	0.0070	0.0198	0.0009
D-Impeller speed	0.0002	0.0743	0.3744	0.6027	0.2901	< 0.0001	< 0.0001	0.0001	0.0006	< 0.0001
E-Particle size	< 0.0001	< 0.0001	< 0.0001	< 0.0001	< 0.0001	< 0.0001	< 0.0001	< 0.0001	< 0.0001	< 0.0001
AB	0.2429	0.3853	0.5140	0.5878	0.9946	0.6120	0.2569	0.1949	0.5992	0.6029
AC	0.7828	0.7502	0.8066	0.9216	0.8297	0.5764	0.7979	0.6122	0.5869	0.4108
AD	0.4155	0.3541	0.3762	0.6565	0.8706	0.0945	0.4034	0.6710	0.6121	0.7815
AE	0.0001	0.0017	0.0090	0.0110	0.2588	0.0640	0.0274	0.0049	0.0007	0.0001
BC	0.4876	0.5809	0.5054	0.5648	0.8491	0.0437	0.1144	0.1849	0.4452	0.5458
BD	0.4190	0.5723	0.5858	0.3521	0.5217	0.6347	0.6399	0.6148	0.8109	0.9308
BE	0.4928	0.5887	0.5270	0.5890	0.8872	0.6939	0.8557	0.7176	0.6883	0.1236
CD	0.1880	0.4036	0.5287	0.5883	0.9505	0.1536	0.3420	0.3708	0.3713	0.1754
CE	0.4891	0.9370	0.9175	0.9730	0.9959	0.6538	0.5202	0.8426	0.7944	0.3370
DE	0.0989	0.1260	0.0279	0.0096	0.0135	0.0018	0.0646	0.0788	0.0918	0.0539

A normal probability plot of the residuals is an important diagnostic tool to detect and explain a systematic departure from the assumption that the errors are normally distributed and independent from each other and that the error variance is homogeneous [29]. A normal probability of the residuals for the entrainment factor after 10 s of flotation, shown in Figure 1, revealed almost no serious violation of the assumptions underlying the analyses, which confirmed the normality of the assumptions and independence of the residuals. All of the above-mentioned considerations indicated the adequacy of the developed relationship. A high value of  $R^2$  (0.9936) indicated a high dependence and correlation between the measured and predicted values of the response. Adjusted R-squared is a modified version of R-squared that has been adjusted for the number of predictors in the model. The adjusted R-squared value increases only if the new term improves the model more than expected by chance, and it decreases when a predictor improves the model by less than expected by chance. Therefore, the adjusted

R-squared value compares the explanatory power of regression models that contain different numbers of predictors [21]. A closely high value of the adjusted correlation coefficient (Adj  $R^2 = 0.9782$ ) showed a high significance of the model; also a total variation of about 98% for the entrainment factor was attributed to the independent variables, and only about 2% of the total variation could not be explained by this model. This fact was also confirmed from the predicted versus observed values plot for cut size, shown in Figure 2. The Pred  $R^2$  value was 0.8884, implying that it could explain the variability in predicting new observations. This was in reasonable agreement with the Adj  $R^2$  value of 0.9782. Adeq precision measures the signal-to-noise ratio; a ratio greater than 4 is desirable [21]. In this investigation, the ratio was 29.09 (Table 5), which indicated an adequate signal. Thus the model could be used to navigate the design space. A similar interpretation can be presented for other responses, as can be seen from the ANOVA results (Table 5).

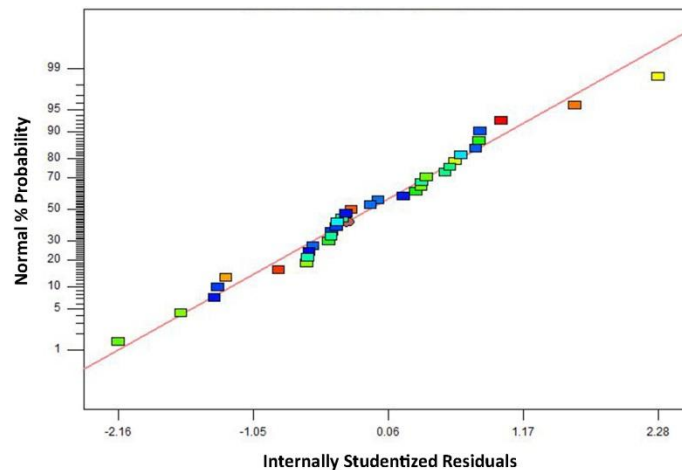


Figure 1. Normal Probability plot of residuals for entrainment factor after 10 s of flotation.

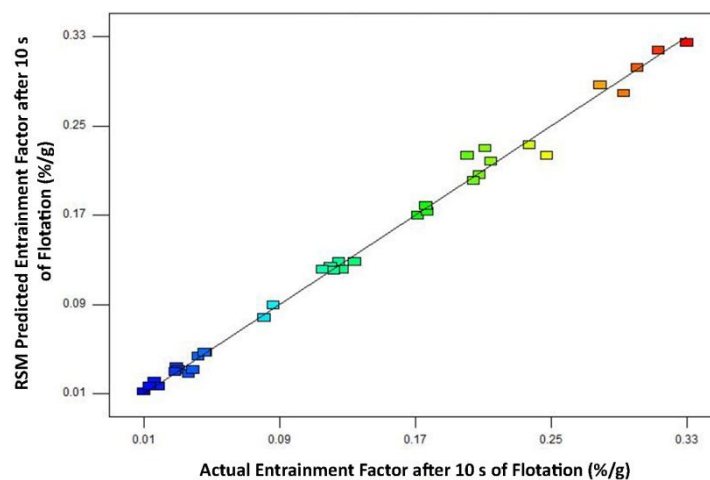


Figure 2. Relation between observed and predicted for entrainment factor after 10 s of flotation.

### 3.2. Effect of solid content

The solid percentage in the pulp has a marked effect on the recovery by entrainment [12, 13]. Figure 3 shows the effects of the solid content on the entrainment factor and water recovery. The effect of solid content can be interpreted either in the equilibrium state related to each individual time or dynamically as the flotation time being elapsed. In the equilibrium state, an unusual effect of the solid content can be observed such that the entrainment factor decreases and water recovery increases as the solid content increases. This is in contrast to the results reported by almost all researchers who have stated that there is a direct correlation between the recovery of suspended solids by entrainment and the water recovered to the concentrate, which is called the hydraulic entrainment mechanism [7, 12, 14, 30-32]. The positive effect of the solid content on water recovery, observed in Figure 3, is in agreement with the results reported by some other investigators [5, 33].

It should first be mentioned that most of the investigations reported in the literature have focused on the entrainment response of slimes (usually smaller than 50  $\mu\text{m}$ ). Under such conditions, the recovery of gangue minerals by entrainment is considered to be often only related to the water recovery because all the mineral particles are perfectly dispersed and mixed in the pulp phase in the flotation cell. Thus it would be expected that the entrainment rate of fine particles increased by solid content following a linear trend [30]. Researches dealing with coarser particles have considered a pulp classification factor such that its value is known to decrease with an increase in particle size, which indicates that the coarse particles tend to settle to the lower portion of a flotation cell, while the fine particles would still be more likely to be uniformly dispersed in the upper portion of the pulp phase. The contribution of entrainment to the recovery of fine and intermediate particles in that region is much larger in the perfectly mixed case than that when the pulp phase is not perfectly mixed. When

significant settling occurs in the flotation cell, the solid percentage in the pulp phase becomes particularly important, as it determines the amount of solids entrained to the concentrate. Thus a

better suspension in the upper portion pulp often leads to more fine particles entering the froth [3, 12].

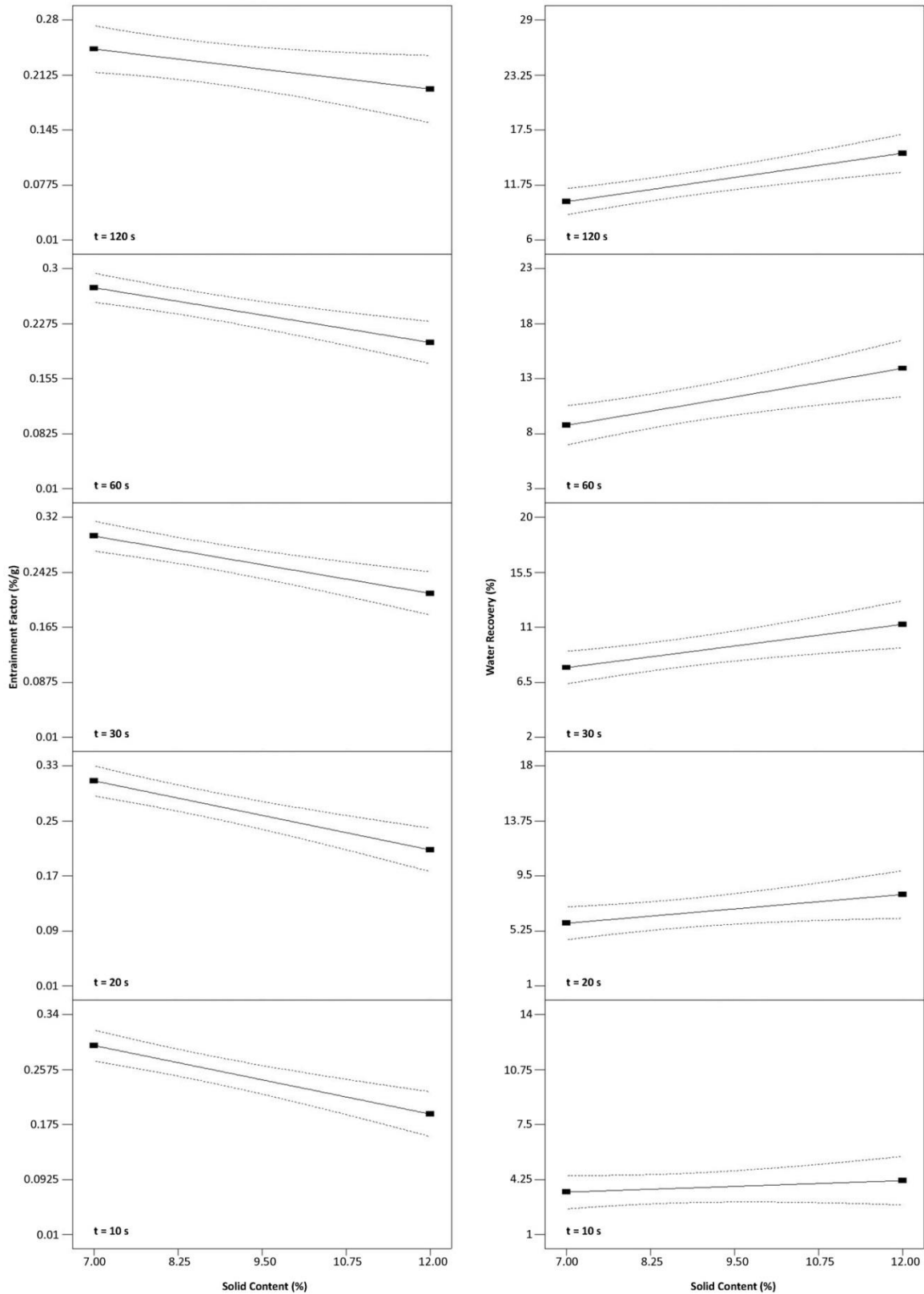


Figure 3. Effects of solid content on entrainment factor and water recovery.

**Table 6. ANOVA results for coal recovery as process response.**

Source	Sum of Squares	df	Mean Square	F value	p-value (Prob > F)
Model	29688.23	20	1484.412	89.03603	< 0.0001
A-Solid content	1.140741	1	1.140741	0.068422	0.7975
B-Collector conc.	134.8552	1	134.8552	8.088711	0.0130
C-Frother conc.	230.2486	1	230.2486	13.81047	0.0023
D-Impeller speed	977.3351	1	977.3351	58.62123	< 0.0001
E-Particle size	24713.99	2	12356.99	741.1811	< 0.0001
AB	19.7366	1	19.7366	1.183815	0.2950
AC	4.519604	1	4.519604	0.271089	0.6107
AD	4.380436	1	4.380436	0.262742	0.6162
AE	265.1602	2	132.5801	7.952244	0.0049
BC	9.853602	1	9.853602	0.591026	0.4548
BD	2.229682	1	2.229682	0.133738	0.7201
BE	105.5114	2	52.75568	3.164322	0.0735
CD	36.37504	1	36.37504	2.1818	0.1618
CE	120.4226	2	60.2113	3.611515	0.0544
DE	1072.502	2	536.2509	32.1647	< 0.0001
Residual	233.4085	14	16.67203		
Lack-of-Fit	170.2486	9	18.91652	1.497512	0.3422
Pure Error	63.15982	5	12.63196		
Cor Total	29921.64	34			

**Table 7. ANOVA results for coal kinetic rate as process response.**

Source	Sum of Squares	df	Mean Square	F value	p-value (Prob > F)
Model	0.037386	20	0.001869	9.939773	< 0.0001
A-Solid content	0.002882	1	0.002882	15.32574	0.0016
B-Collector conc.	2.16E-05	1	2.16E-05	0.115117	0.7394
C-Frother conc.	0.000278	1	0.000278	1.480482	0.2438
D-Impeller speed	0.004476	1	0.004476	23.80106	0.0002
E-Particle size	0.025267	2	0.012634	67.17689	< 0.0001
AB	0.000158	1	0.000158	0.839862	0.3750
AC	9.36E-06	1	9.36E-06	0.049753	0.8267
AD	3.59E-05	1	3.59E-05	0.190651	0.6690
AE	0.000966	2	0.000483	2.56726	0.1122
BC	8.21E-05	1	8.21E-05	0.436634	0.5195
BD	6.86E-06	1	6.86E-06	0.03646	0.8513
BE	0.000153	2	7.64E-05	0.406315	0.6737
CD	5.22E-05	1	5.22E-05	0.277732	0.6064
CE	5.27E-05	2	2.64E-05	0.140182	0.8704
DE	0.002764	2	0.001382	7.348234	0.0066
Residual	0.002633	14	0.000188		
Lack-of-Fit	0.001612	9	0.000179	0.87765	0.5936
Pure Error	0.001021	5	0.000204		
Cor Total	0.040019	34			

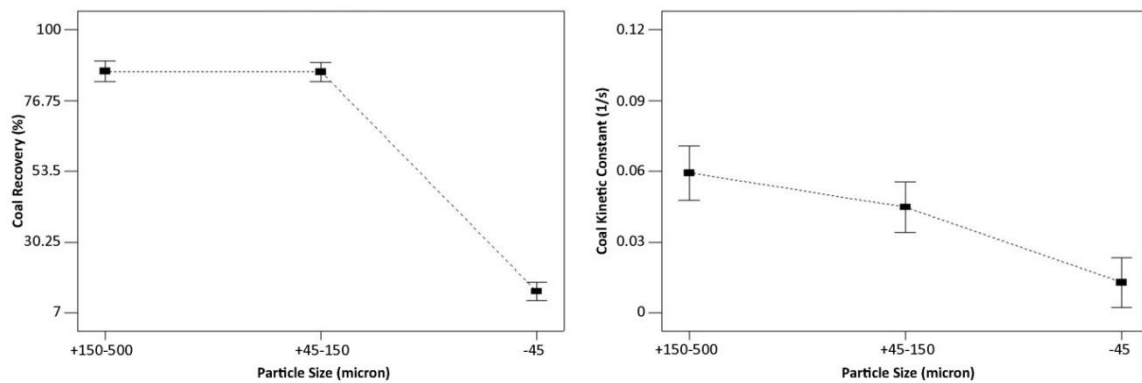


**Figure 4. Effect of particle size on coal recovery and kinetic rate.**

The observed unusual effect of the solid content on the entrainment factor can be interpreted by referring to the distribution of coal and ash in different size fractions of the coal sample used in this work. As given in Table 1, ash materials are mostly included in fine fractions of the samples; therefore, coarse particles are expected to yield a higher flotation rate than fine particles. To confirm this expectation, the experimental design of Table 3 was also analyzed for final coal recovery and kinetics rate as the process responses. The ANOVA results for coal recovery and kinetics rate are given in Tables 6 and 7, respectively. As it can be seen, the effect of particle size on both responses is significant. For an easier interpretation, the main effects of particle size are shown in Figure 4. It clearly shows that coal recovery and kinetics rate of coarse particles are considerably higher than fine particles. Under this condition, the accumulation of coarse particles in the upper portion of pulp is due to their higher flotation rate as well as lower density, and consequently, a lower settling rate, which provides a non-perfectly mixed condition in the pulp phase and prevents the fine particles from entraining to the froth zone. A low  $p$ -value for the interaction effect between the solid content and particle size parameters (AE) given in Table 5 confirms the proposed interpretation.

From the dynamic viewpoint, the effect of solid content on the entrainment factor decreases with time such that the effect becomes insignificant after 120 s, i.e. when the flotation process finished (see  $p$ -values given in Table 5). At the earlier flotation times, a high flotation rate of particles increases the entrainment of fine particles by swarm mechanism (as will be discussed later); but the entrainment factor decreases as the solid content and floatable particle concentration decrease with increase in the flotation time. Similar results have also been reported by Neethling and Cilliers [32]. However, water recovery continuously increases as the flotation process progresses (see  $p$ -values given in Table 5). The same reasoning as given for the entrainment factor response can be stated for the increasing trend of water recovery with time. As mentioned earlier, the rate of solid recovery is high at the start of flotation and decreases with an increase in the flotation time; therefore, the swarm of floatable particles first prevents water to rise to

the froth zone and then water recovery tends to gradually increase with decrease in the solid content due to the froth stabilizing action. The effect of frother on responses is discussed later in this paper.

### 3.3. Effect of collector concentration

The effects of the collector concentration on the entrainment factor and water recovery are shown in Figure 5. This figure and the  $p$ -values given in Table 5 indicate that the effect of the collector concentration on responses is not significant and can be neglected. The main reason for the insignificant effect of the collector concentration variation on responses can be attributed to the chemical structure of the collector used. Diesel oil is a non-ionic collector that interacts with coal-bearing particles through Van der Waals bindings. In contrast, it would be expected that diesel oil is not adsorbed at the polar surface of ash materials. Thus a change in the collector concentration does not influence the entrainment of ash particles by non-selective flotation. In addition, diesel oil is a non-polar substance and does not dissolve in water, and thus it actually has no frothing property [34]. Hence, it would be expected that changing the collector concentration does not directly affect the water recovery by the frother-stabilizing mechanism. However, time dependent variations of  $p$ -values show that an increase in the collector concentration may negatively influence the entrainment factor but water recovery is directly influenced by time. At the equilibrium condition, as the collector concentration increases, more locked particles are activated and tend to float to froth. Therefore, the entrainment factor shows a fair increase as the collector concentration is increased. As the flotation time is elapsed, the solid content of pulp decreases. Therefore, a low solid concentration with a higher collector consumption produces higher-recovery products with a lower-ash content instead of lower-recovery products with a higher-ash content obtained at a higher solid density with a lower collector. Figure 6 shows the main effect of coal recovery against collector concentration (see Table 6). Akdemir and Sönmez [11] have also reported similar results. A fair improvement in water recovery with time can be attributed to the stabilizing effect of the frother as the solid content decreases.

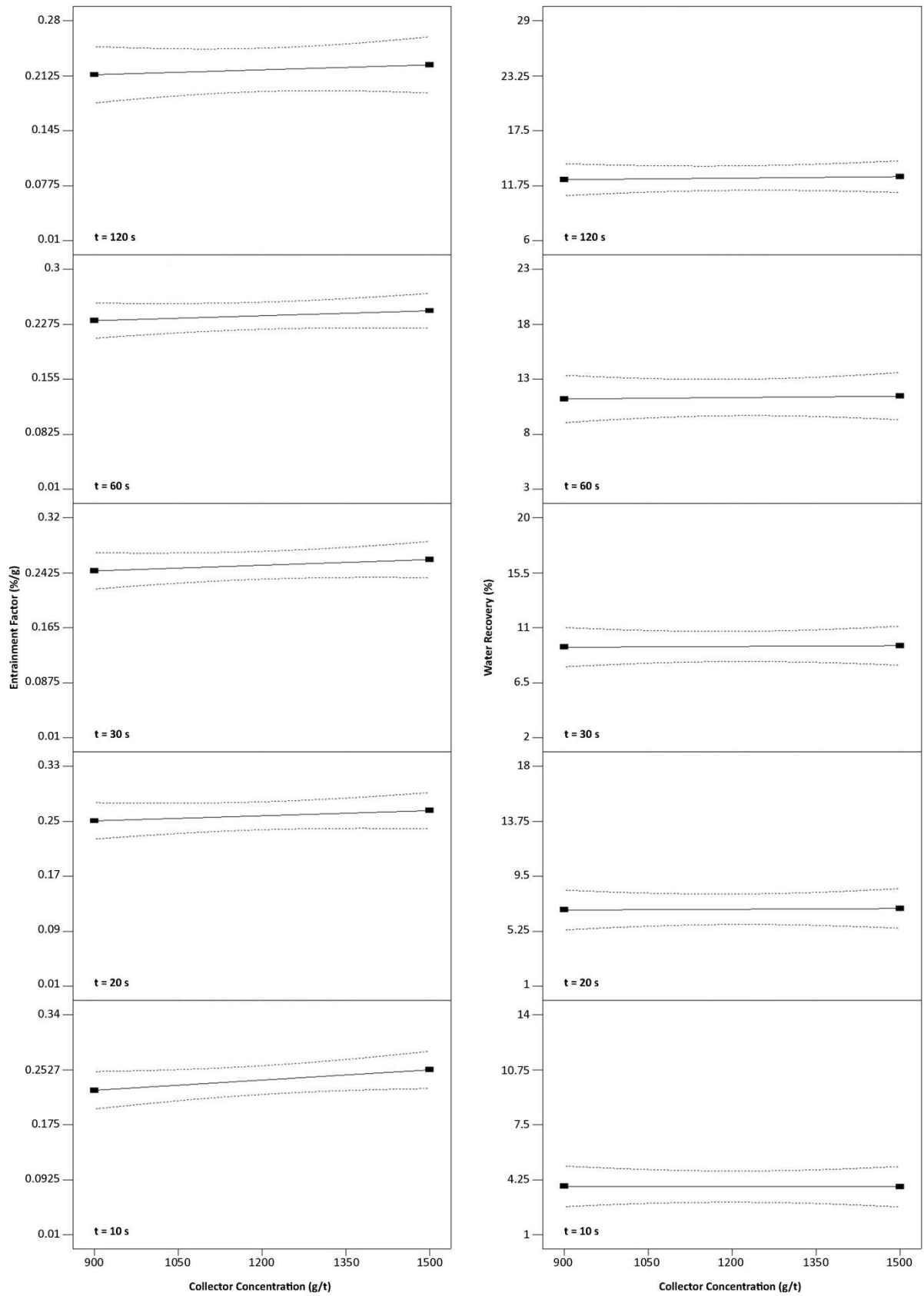


Figure 5. Effect of collector concentration on entrainment factor and water recovery.

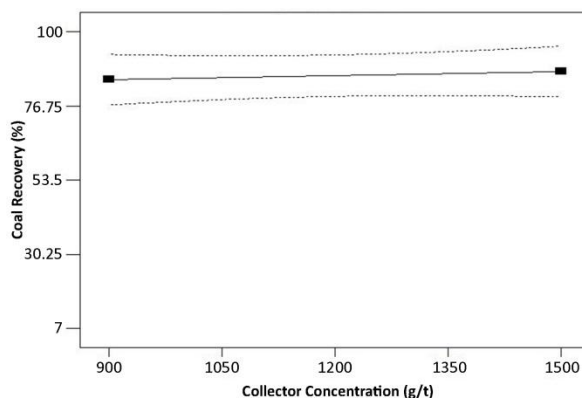


Figure 6. Effect of collector concentration on final coal recovery.

### 3.4. Effect of frother concentration

Figure 7 shows the effects of the frother concentration on the entrainment factor and water recovery. The ANOVA results tabulated in Table 5 indicate that the effect of changing the frother concentration on the entrainment factor is insignificant. The effects of the frother type and concentration on the gangue entrainment has been investigated by few researchers, who showed that frothers had no effect on the relationship between particle entrainment and water recovery [4, 35]. In contrast, water recovery gradually improved by the frother concentration from both the equilibrium and dynamic viewpoints (Table 5 and Figure 7). It is well-known that particles are the main factor stabilizing three-phase froths. They prevent bubbles coming into contact and coalesce together [36]. At the initial times of flotation up to about 30 s, while the flotation recovery is still considerable, the froth zone is highly stable due to the high solid concentration therein. Afterwards, as the solid concentration of pulp decreases, the froth zone approaches the foam state, in which frothers are the dominant stabilizing factor [17, 37-41]. Bubbles in foam have a thicker liquid film with higher water content so that the water recovery increases with time. The stabilization mechanisms of froth and foam are schematically illustrated in Figure 8. Visual observation, as shown in Figure 9, also indicated that the compact structure of the froth at initial flotation times gradually changed to a looser structure froth phase with larger bubbles at the middle stages of flotation, and finally, to a stable wet foam.

### 3.5. Effect of impeller speed

The effects of impeller speed on the entrainment factor and water recovery are shown in Figure 10. As seen, the entrainment factor slightly increases by raising the impeller speed at the initial flotation times and then the trend inversely changes as the flotation process goes on.

It has been shown that the recovery of mineral particles by entrainment is influenced by the impeller speed [11, 33, 42, 43]. In a flotation cell, the function of the impeller is to increase the chances of collision between the bubbles and mineral particles, and to make both solids and air fully dispersed and mixed in the pulp phase. At short flotation times, due to a higher solid content of the pulp, increasing the agitation rate provides the momentum for particles and bubbles to collide with each other, and consequently, more ash is entrained to the concentrate. As the solid content of the pulp decreases by flotation time, excessive agitation rate can change the solid suspension and the pulp density in the region below the pulp/froth interface. It can also provide more turbulence to the froth, which negatively affects the froth stability, and consequently, leads to the resulting decreased entrainment rate [11].

The *p*-values for the water recovery response, given in Table 5, indicate that the effect of impeller speed on water recovery is positively significant at any flotation time-step. This direct correlation between the impeller speed and water recovery can be attributed to the increase in the numerical density of air bubbles per volume of pulp. Therefore, the increase in the gas rate will inevitably carry over a greater amount of water to the froth phase from the pulp phase. In addition, the continuous entering of bubbles into the froth prevents the feed water in the froth to drain back into the pulp [1].

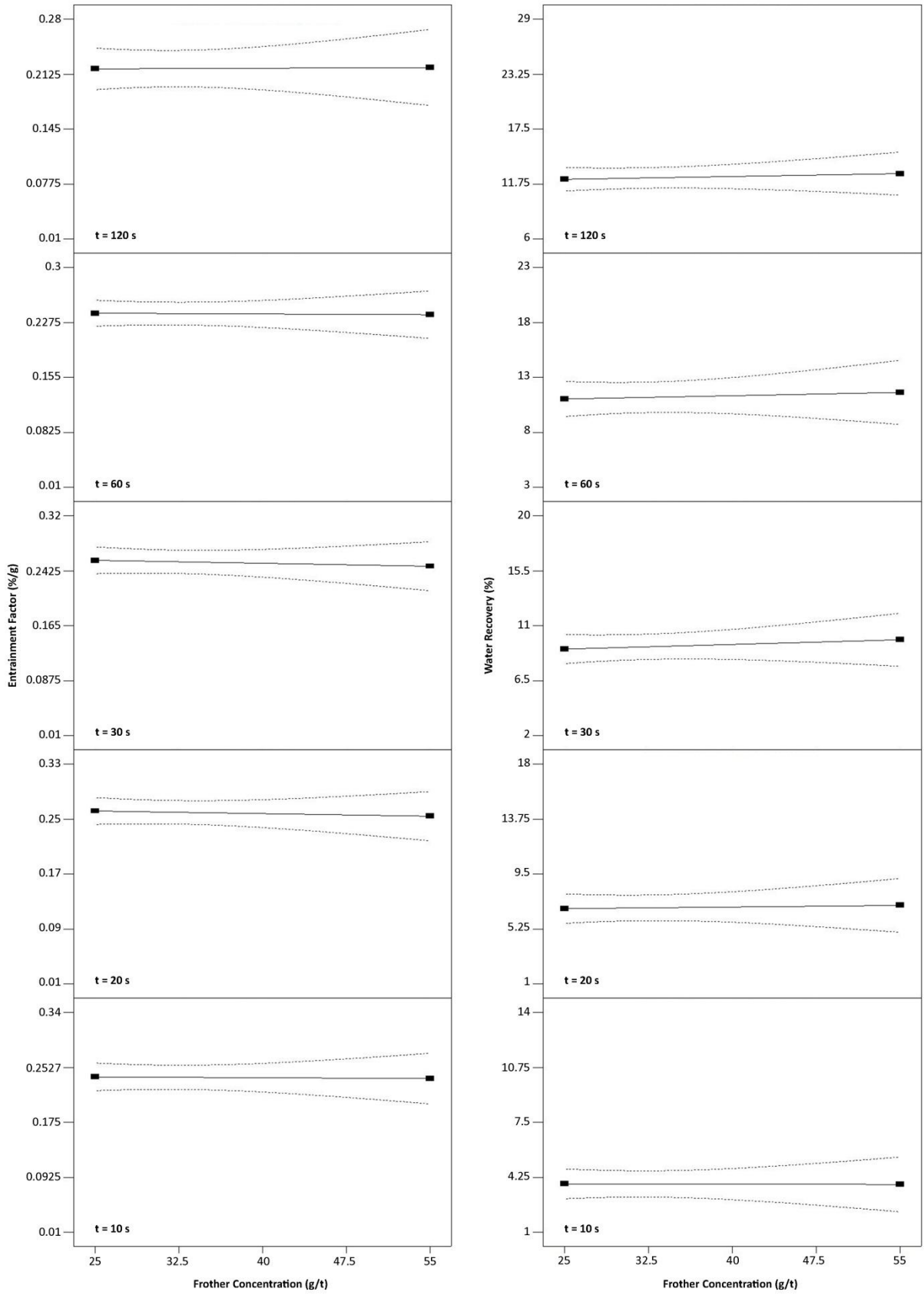


Figure 7. Effects of frother concentration on entrainment factor and water recovery.

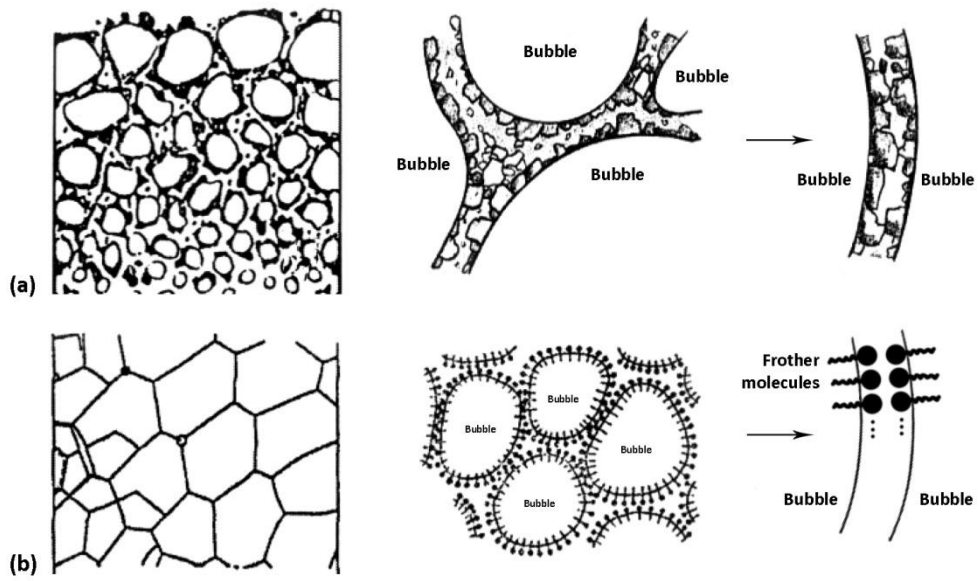


Figure 8. Comparison between stabilization mechanism in froth (a) and foam (b) phases ([38], modified).

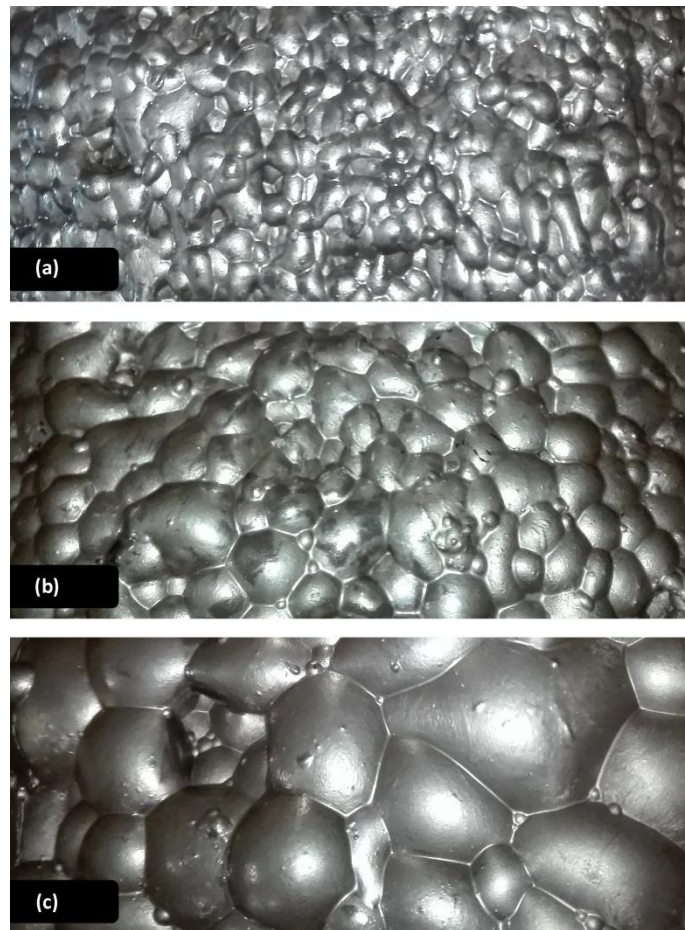


Figure 9. Change in structure of froth during coal flotation test after (a) 30 s, (b) 60 s, and (c) 120 s.

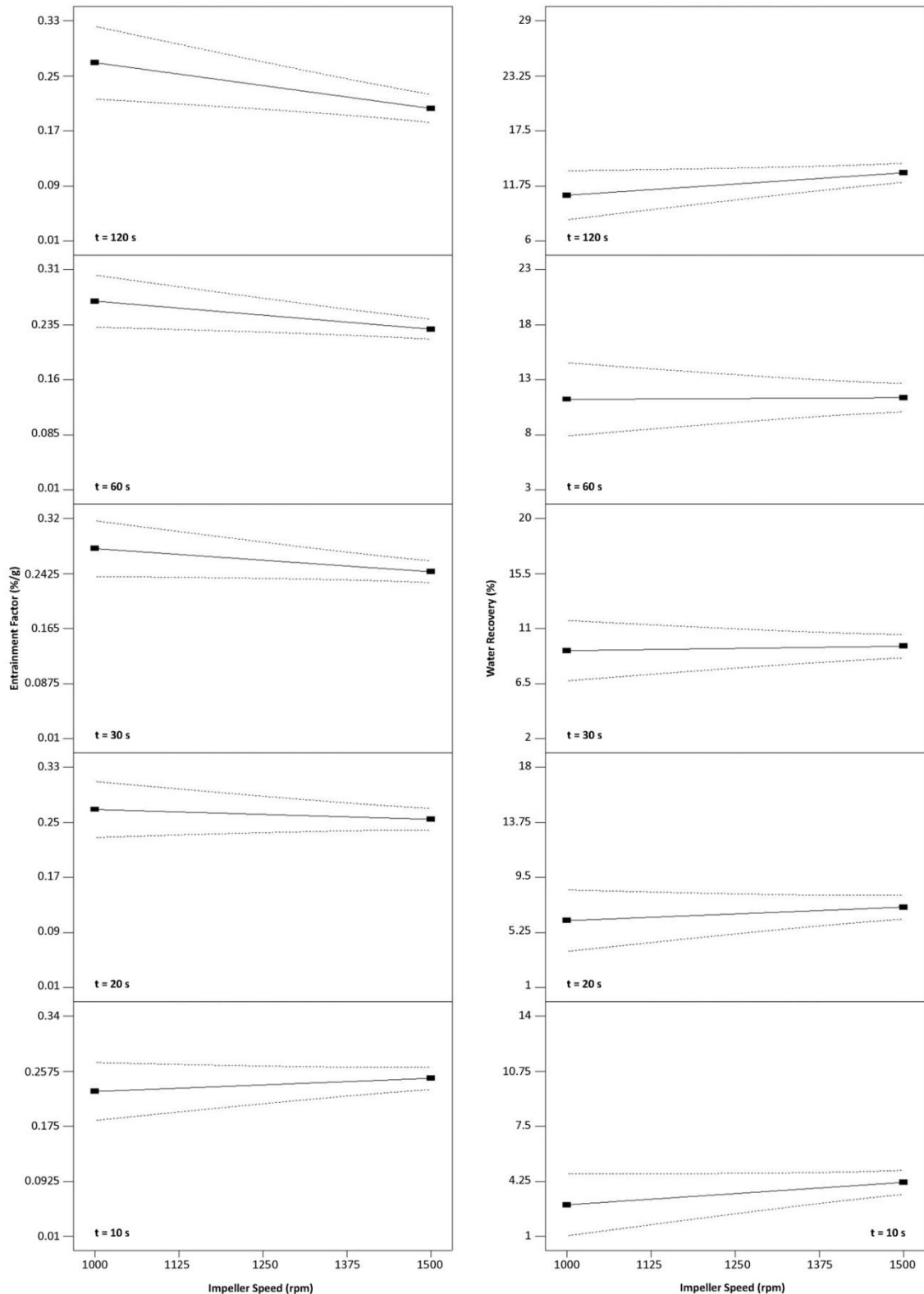


Figure 10. Effect of impeller speed on entrainment factor and water recovery.

### 3.6. Effect of particle size

Figure 11 shows the effects of particle size on the entrainment factor and water recovery. Figure 11 and the ANOVA results listed in Table 5 clearly indicate that the particle size has a marked effect on both the entrainment rate and water recovery.

The key point in Figure 11 is the direct correlation between the entrainment rate and particle size such that the entrainment factor increases as the particle size increases. These results are in contrast to those reported by almost all the other researchers as the recovery of hydrophilic

minerals by entrainment increases as the particle size decreases [8, 11, 16, 19, 20, 43, 44]. They have denoted that in the pulp phase, fine particles are easily suspended in the water or the water film

surrounding the bubbles in the region below the pulp/froth interface compared with coarse particles, and hence, they have more chance to travel up through the froth to the concentrate.

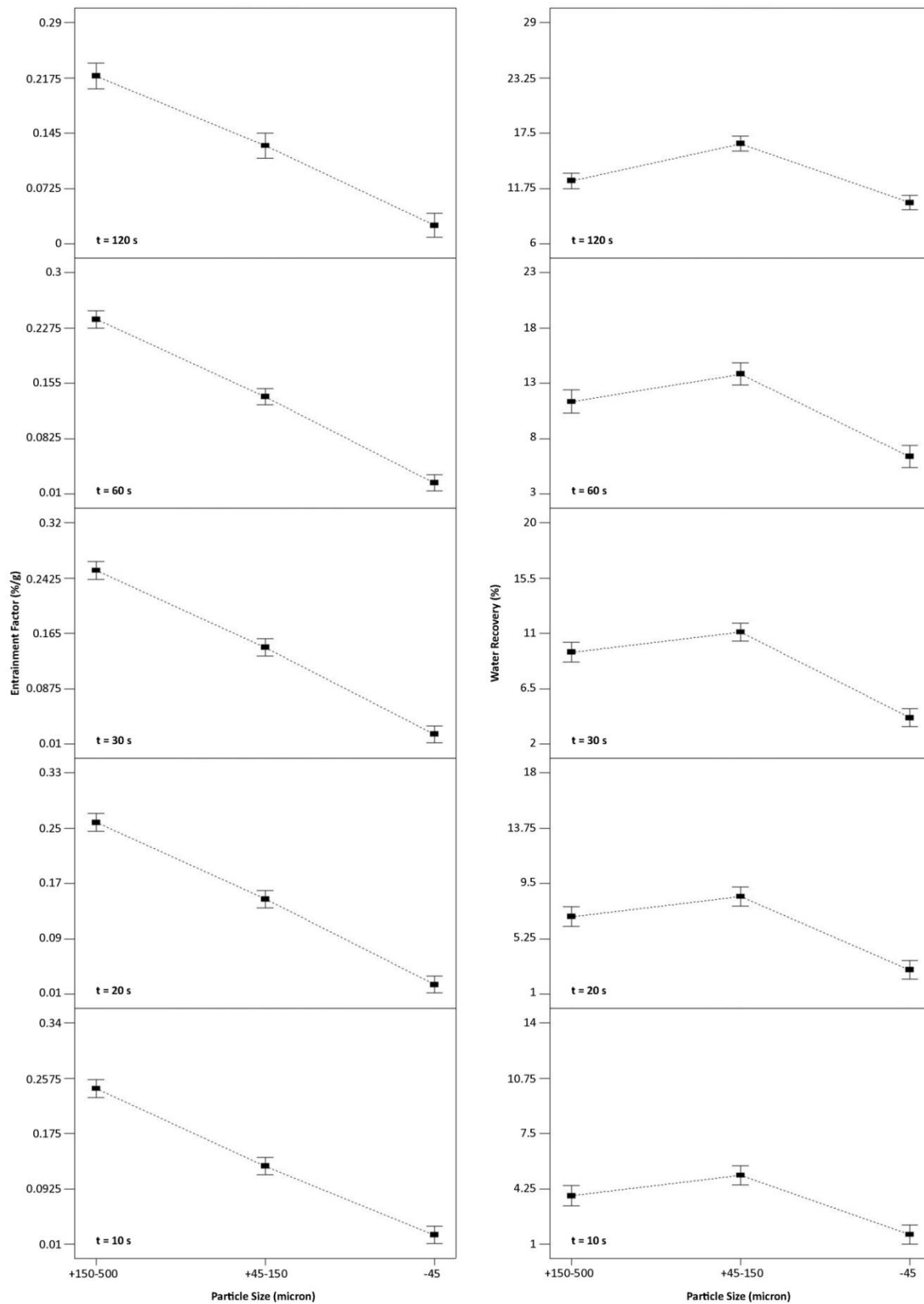


Figure 11. Effect of particle size on entrainment factor and water recovery.

Numerous reasons can be presented to interpret the unusual effect of particle size on the entrainment rate, as observed in this study. The most important reason can be attributed to the density difference between the coal and ash materials. However, few researchers have denoted that particle density, also known as mineral specific gravity, can be a factor affecting entrainment [8, 45, 46]. It has been demonstrated that the particles with a lower density have a higher entrainment rate because they tend to move with water to the froth zone due to their low sedimentation velocities. Smith and Warren [8] took advantage of the Stokes' law to demonstrate the sedimentation rates expected for different density minerals in the pulp of a flotation cell, showing that those particles with a higher density settle more quickly and have less chance to be transported to the concentrate. Tests conducted by Drzymala [46] have suggested that the effect of particle density on the degree of entrainment would be very strong. Given the density values 1.2-1.24 for coal and 3.2-3.8 for ash materials (as measured in the laboratory), and also the higher ash content of finer particle size fraction (Table 1), it can be stated that fine particles would have a higher settling rate than coarse particles, and thus the entrainment rate decreases as the particle size decreases.

A higher coal portion of coarse particle size fractions (Table 1) enhances the flotation rate of coarse particles over the fine ones, as shown in Figure 4. Under these conditions, the entrainment can dominantly be caused by the swarm mechanism. To date, three mechanisms have been proposed to characterize the mineral particles in the flotation cell travelling across the pulp/froth interface from the pulp to the froth by entrainment. They are boundary layer theory, bubble wake theory, and bubble swarm theory. In the boundary layer theory, mineral particles are transported to the froth phase in the bubble lamella, i.e. the thin hydrodynamic layer of water surrounding the bubble [47, 48], while in the bubble wake theory, water including the mineral particles is transported to the froth phase in the wake of an ascending bubble [49]. According to the literature, these two mechanisms are mostly accepted as responsible for the gangue recovery by many researchers who have used them to interpret the effect of operating factors on flotation responses in their observations. The third mechanism, i.e. swarm theory that have received less attention, was first proposed by Smith and Warren [8]. Based on the swarm theory, while

bubbles are travelling up through the cell, the region below the froth/pulp interface is congested with bubbles as the bubbles slow down and crowd together. Because of drainage through the rising bubble swarm, some water including the suspended solids drops back, while some other water including the suspended solids is squeezed upwards due to the buoyancy of the bubble swarm. Afterwards, as each layer of bubbles is pushed up, another layer of bubbles will form. In this way, more solids suspended in the water are pushed up to the froth. Coarser fractions of particle sizes have a better floatability due to a higher coal content and a lower density. Therefore, it would be expected that more ash particles are entrapped between rising coarse coal particle/bubble regime. Figure 12 schematically demonstrates the transportation of bubbly regime including the suspended particles to the froth from the pulp phase based on the bubble swarm theory. The proposed reason can be proved by referring to the coal recovery, entrainment rate, and water recovery plots against the flotation time. Figure 13 shows the aforesaid plots for different particle size fractions. As seen in Figure 13, the entrainment factor follows the same trend as the coal recovery. In the case of coarse fraction, the entrainment rate increases up to about 30 s of flotation due to the swarm mechanism enhanced by the higher flotation rate of coarse particles, and then decreases as the coal recovery decreases because the concentration of floatable particles decreases by time. In contrast, fine particles follow an increasing trend for both the recovery and entrainment rate. The same trend of water recovery, in this case, can lead us to conclude that the entrainment of fine particles is mainly caused by the bubble wake theory as well as, possibly, the boundary layer theory rather than the swarm mechanism.

The improvement of froth stability can be stated as another reason for the higher entrainment factor in the presence of coarse particles. It has been shown that the amount of entrained gangue reporting to the concentrate can be affected by the froth structure [19, 20, 32]. The froth structure is very complicated, and it is dependent on a number of factors including water content, gas rate, bubble size, content of hydrophobic particles, and concentration and type of frothers. When there is a change in these contributing factors, the froth structure such as the thickness of the lamellae and the length of Plateau borders changes; the froth structure influences the water content in the froth and then affects the water recovery and recovery

by entrainment. A loose froth structure, which is conducive to the motion of water, definitely influences the amount of gangue minerals entrained to the concentrate. Froth stability is a measure of froth structure, and it refers to the rate of bubble coalescence and bubble bursting. Basically, a froth with a relatively low coalescence and small bubbles not only allows the recovery of attached particles but also promotes the recovery of gangue minerals by entrainment [3]. The structure of the froth phase after 30 s of flotation of different particle size fractions is shown in Figure 14. It is obviously observed in this figure that fine particles produce a significantly looser structure froth phase with

larger bubbles. Therefore, the increased entrainment rate and water recovery by coarse particles can be attributed to the improved froth stability and structure.

A slight decrease in the entrainment factor by time can be ascribed to a gradual decrease in the solid content of the pulp, as described in the earlier sections. At equilibrium conditions, the improved water recovery by increasing the particle size comes from the froth stabilizing effect thereof. From a dynamic viewpoint, especially after 30 s of flotation, the slight increase in water recovery is due to the effect of frother instead of solid particles.

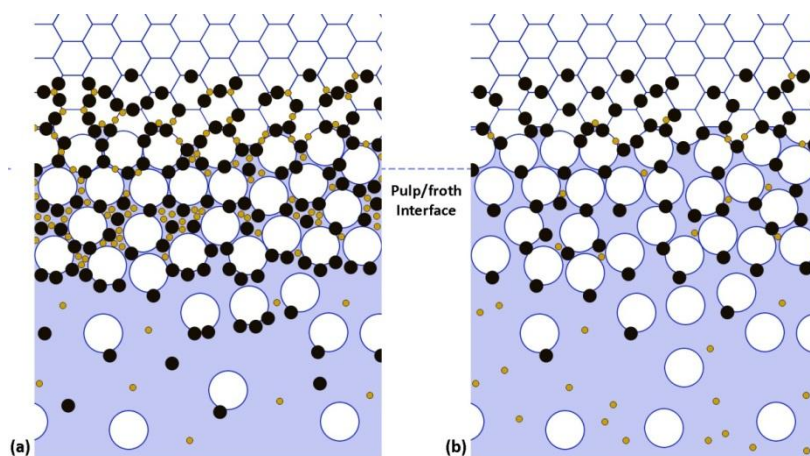


Figure 12. Schematic illustration of swarm theory in coarse particle flotation as proposed in this study: (a) before 30 s, and (b) after 30 s.

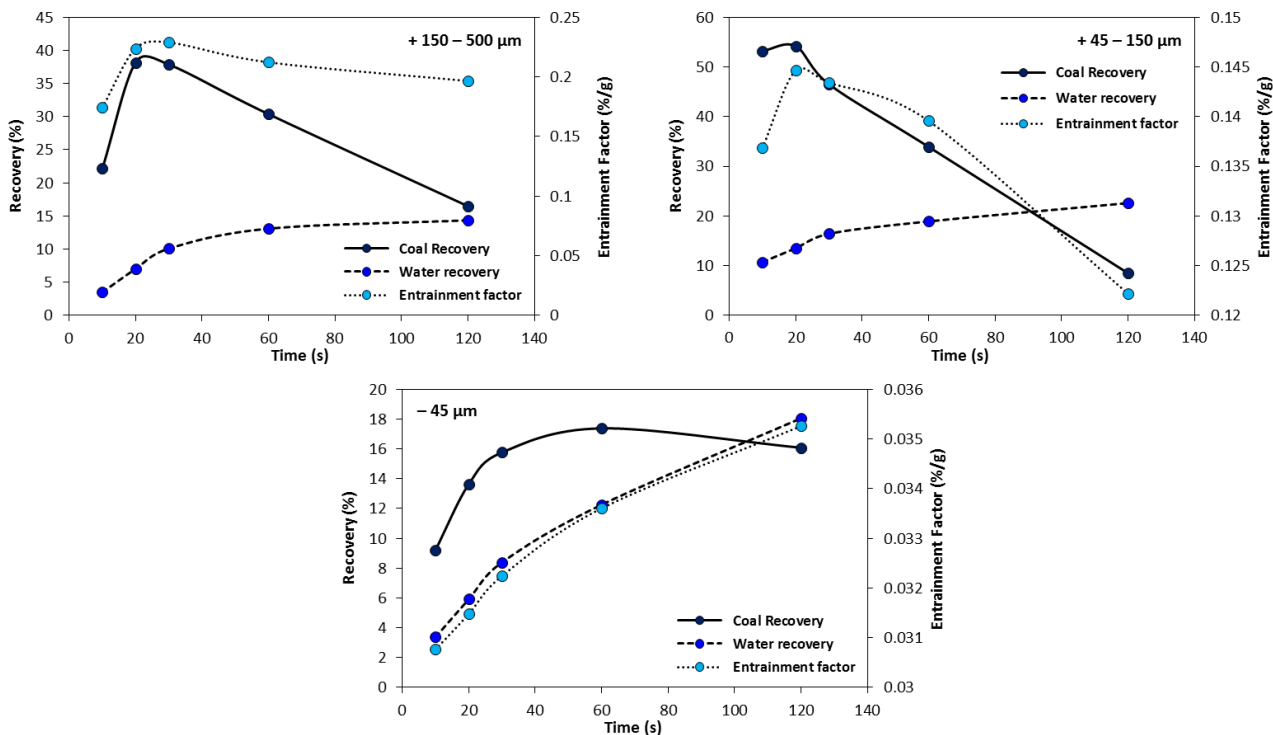
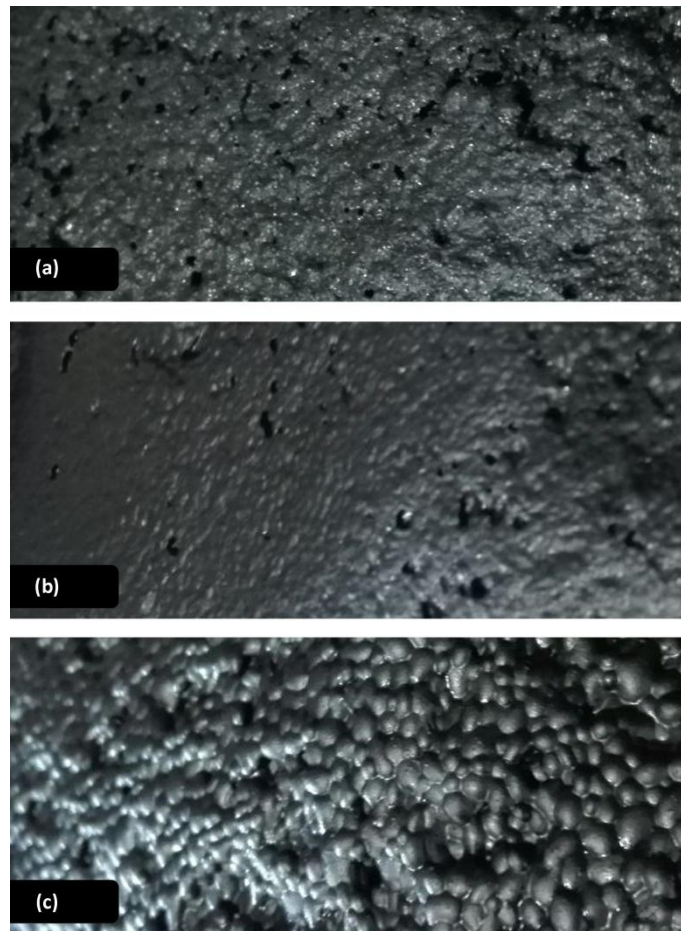


Figure 13. Time-step plots of coal recovery, entrainment factor, and water recovery for different particle size fractions.



**Figure 14.** Effect of particle size on froth structure before about 30 s of flotation: (a) +150-500  $\mu\text{m}$ , (b) +45-150  $\mu\text{m}$ , and (c) -45  $\mu\text{m}$ .

#### 4. Conclusions

In any coal flotation process, entrainment is of great importance in the recovery of ash materials, and has a significant effect on the selectivity and efficiency of the process. Though the influence of different operating and hydrodynamic factors such as water recovery, pulp density, particle size distribution, froth height, froth structure, impeller speed, gas rate, particle density, froth retention time, and flotation cell design on entrainment, the behavior was investigated in the literature but the significance of continuity and time-dependency of the flotation process needs to be explored. In this work, a systematic investigation was statistically designed to assess the effect of the key operating factors on the entrainment behavior of a sample coal flotation. The variations in the entrainment factor of ash materials and water recovery at different flotation times were analyzed as the experimental responses. The results obtained showed that the effects of the studied factors would change as the flotation time elapsed. In addition, it was also shown that the entrainment mechanism was a function of the flotation time as

well as the water recovery, state of solid suspension in the pulp, and degree of drainage in the froth, as denoted in the literature.

#### Acknowledgments

Technical supports of Zarand Coal Washing Plant (Zarand, Iran) and INVENTIVE<sup>®</sup> Mineral Processing Research Center (Zarand, Iran) are acknowledged.

#### References

- [1]. Cilek, E.C. and Yilmazer, B.Z. (2003). Effects of hydrodynamic parameters on entrainment and flotation performance. *Minerals Engineering*. 16: 745-756.
- [2]. Ross, V.E. (1990). Flotation and entrainment of particles during batch flotation tests. *Minerals Engineering*, 3(3/4): 245-256.
- [3]. Wang, L., Peng, Y., Runge, K. and Bradshaw, D. (2015). A review of entrainment: Mechanisms, contributing factors and modelling in flotation. *Minerals Engineering*. 70: 77-91.
- [4]. Trahar, W.J. (1981). A rational interpretation of the role of particle size in flotation. *International Journal of Mineral Processing*. 8: 289-327.

- [5]. Warren, L.J. (1985). Determination of the contributions of true flotation and entrainment in batch flotation tests. *International Journal of Mineral Processing*. 14: 33-44.
- [6]. Kirjavainen, V.M. (1989). Application of a probability model for the entrainment of hydrophilic particles in froth flotation. *International Journal of Mineral Processing*. 27: 63-74.
- [7]. Kirjavainen, V.M. (1996). Review and analysis of factors controlling the mechanical flotation of gangue minerals. *International Journal of Mineral Processing*. 46: 21-34.
- [8]. Smith, P.G. and Warren, L.J. (1989). Entrainment of particles into flotation froths. *Mineral Processing & Extractive Metallurgy Review*. 5: 123-145.
- [9]. Savassi, O.N., Alexander, D.J., Franzidis, J.P. and Manlapig, E.V. (1998). An empirical model for entrainment in industrial flotation plants. *Minerals Engineering*. 11: 243-256.
- [10]. Shi, F.N. and Zheng, X.F. (2003). The rheology of flotation froths. *International Journal of Mineral Processing*. 69 (1-4): 115-128.
- [11]. Akdemir, Ü. and Sönmez, I. (2003). Investigation of coal and ash recovery and entrainment in flotation. *Fuel Processing Technology*. 82: 1-9.
- [12]. Zheng, X., Johnson, N.W. and Franzidis, J.P. (2006). Modelling of entrainment in industrial flotation cells: water recovery and degree of entrainment. *Minerals Engineering*. 19: 1191-1203.
- [13]. Yianatos, J., Contreras, F., Díaz, F. and Villanueva, A. (2009). Direct measurement of entrainment in large flotation cells. *Powder Technology*. 189: 42-47.
- [14]. Yianatos, J. and Contreras, F. (2010). Particle entrainment model for industrial flotation cells. *Powder Technology*. 197: 260-267.
- [15]. Konopacka, Z. and Drzymala, J. (2010). Types of particles recovery-water recovery entrainment plots useful in flotation research. *Adsorption*. 16: 313-320.
- [16]. Wiese, J., Becker, M., Yorath, G. and O'connor, C. (2015). An investigation into the relationship between particle shape and entrainment. *Minerals Engineering*. 83: 211-216.
- [17]. Kracht, W., Orozco, Y. and Acuña, C. (2016). Effect of surfactant type on the entrainment factor and selectivity of flotation at laboratory scale. *Minerals Engineering*. 92: 216-220.
- [18]. Little, L., Wiese, J., Becker, M., Mainza, A. and Ross, V. (2016). Investigating the effects of particle shape on chromite entrainment at a platinum concentrator. *Minerals Engineering*. 96-97: 46-52.
- [19]. Wiese, J.G. and O'connor, C.T. (2016). An investigation into the relative role of particle size, particle shape and froth behaviour on the entrainment of chromite. *International Journal of Mineral Processing*. Article In Press.
- [20]. Lima, N.P., Pinto, T.C.S., Tavares, A.C. and Sweet, J. (2016). The entrainment effect on the performance of iron ore reverse flotation. *Minerals Engineering*. 96-97: 53-58.
- [21]. Montgomery, D.C. (2013). *Design and Analysis of Experiments*. 8<sup>th</sup> ed., John Wiley & Sons, Inc., New York.
- [22]. Azizi, A. (2015). Optimization of rougher flotation parameters of the Sarcheshmeh copper ore using a statistical technique. *Journal of Dispersion Science and Technology*. 36 (8): 1066-1072.
- [23]. Atkinson, A.C., Donev, A.N. and Tobias, R.D. (2007). *Optimum Experimental Designs with SAS*, Oxford University Press, London.
- [24]. Triefenbach, F. (2008). *Design of Experiments: The D-Optimal Approach and Its Implementation As a Computer Algorithm*. BSc. Thesis in Information and Communication Technology. Sweden.
- [25]. Cornell, J.A. (1990). *How to Apply Response Surface Methodology*, 2<sup>nd</sup> ed., American Society for Quality Control, Wisconsin.
- [26]. Wills, B.A. and Finch, J.A. (2016). *Wills' Mineral Processing Technology*. 8<sup>th</sup> ed., Elsevier, England.
- [27]. Mehrabani, J.V., Noaparast, M., Mousavi, S.M., Dehghan, R., Rasooli, E. and Hajizadeh, H. (2010). Depression of pyrite in the flotation of high pyrite low-grade lead-zinc ore using *Acidithiobacillus ferrooxidans*. *Minerals Engineering*. 23: 10-16.
- [28]. Clarke, G.M. and Kempson, R.E. (1997). *Introduction to the Design and Analysis of Experiments*, Arnold, London.
- [29]. Yetilmezsoy, K., Demirel, S. and Vanderbei, R.J. (2009). Response surface modeling of Pb(II) removal from aqueous solution by *Pistacia vera* L.: Box-Behnken experimental design. *Journal of Hazardous Materials*. 171: 551-562.
- [30]. Engelbrecht, J.A. and Woodburn, E.T. (1975). The effect of froth height, aeration rate and gas precipitation on flotation. *Journal of South African Institute of Mining & Metallurgy*. 10: 125-132.
- [31]. Laplante, A., Kaya, M. and Smith, H. (1989). The effect of froth on flotation kinetics- a mass transfer approach. *Mineral Processing & Extractive Metallurgy Review*. 5: 147-168.
- [32]. Neethling, S.J. and Cilliers, J.J. (2009). The entrainment factor in froth flotation: model for particle size and other operating parameter effects. *International Journal of Mineral Processing*. 93: 141-148.

- [33]. Cileck, E.C. (2009). The effect of hydrodynamic conditions on true flotation and entrainment in flotation of a complex sulphide ore. *International Journal of Mineral Processing*. 90: 35-44.
- [34]. Guard, H.E., NG, J. and Laughin, R.B. (1983). Characterization of Gasolines, Diesel Fuels & Their Water Soluble Fractions. Naval Biosciences Laboratory, USA.
- [35]. Rahal, K., Manlapig, E. and Franzidis, J.P. (2001). Effect of frother type and concentration on the water recovery and entrainment recovery relationship. *Minerals & Metallurgical Processing*. 18: 138-141.
- [36]. Khoshdast, H. and Sam, A. (2011). Flotation frothers: review of their classifications, properties and preparation. *The Open Mineral Processing Journal*. 4: 25-44.
- [37]. Kitchener, J.A. and Cooper, C.F. (1959). Current concepts in the theory of foaming. *Quantitative Review*. 13: 71-97.
- [38]. Klassen, V.I. and Mokrousov, V.A. (1963). *An Introduction to the Theory of Flotation*, Butterworth, London.
- [39]. Grau, R.A., Laskowski, J.S. and Heiskanen, K. (2005). Effect of frothers on bubble size. *International Journal of Mineral Processing*. 76 (4): 225-233.
- [40]. Finch, J.A., Nasset, J.E. and Acuña, C. (2008). Role of frother on bubble production and behaviour in flotation. *Minerals Engineering*. 21 (12): 949-957.
- [41]. Kracht, W. and Finch, J. (2009). Bubble break-up and the role of frother and salt. *International Journal of Mineral Processing*. 92 (3): 153-161.
- [42]. Schubert, H. (1999). On the turbulence-controlled microprocesses in flotation machines. *International Journal of Mineral Processing*. 56: 257-276.
- [43]. Nguyen, A.V. and Schulze, H.J. (2004). *Colloidal science of flotation*. Surfactant Science Series, Vol. 118. Marcel Dekker Inc., New York, pp. 709-775.
- [44]. Lynch, A., Johanson, N., Manlapig, E. and Thorne, C. (1981). *Mineral and Coal Flotation Circuits*, Elsevier, Amsterdam.
- [45]. Maachar, A. and Dobby, G.S. (1992). Measurement of feed water recovery and entrainment solids recovery in flotation columns. *Canadian Metallurgical Quarterly*. 31: 167-172.
- [46]. Drzymala, J. (1994). Characterization of materials by Hallimond tube flotation. Part 1: Maximum size of entrained particles. *International Journal of Mineral Processing*. 42: 139-152.
- [47]. Moys, M.H. (1978). A study of a plug-flow model for flotation froth behaviour. *International Journal of Mineral Processing*. 5: 21-38.
- [48]. Hemmings, C. (1981). On the significance of flotation froth liquid lamella thickness. *Transactions of the Institution of Mining and Metallurgy*. 90: C96-C102.
- [49]. Yianatos, J., Finch, J. and Laplante, A. (1988). Selectivity in column flotation froths. *International Journal of Mineral Processing*. 23: 279-292.

## تأثیر پارامترهای عملیاتی بر رفتار وابسته به زمان دنباله‌روی خاکستر در فلوتاسیون یک نمونه زغال سنگ

حسین پاریاد، حمید خوشدست و وحیده شجاعی\*

بخش مهندسی معدن، مجتمع آموزش عالی زرنند، ایران

ارسال ۲۰۱۶/۱۱/۱۶، پذیرش ۲۰۱۷/۱/۲۸

\* نویسنده مسئول مکاتبات: v.shojaei@uk.ac.ir

---

### چکیده:

دنباله‌روی ذرات به کف یک عامل بسیار مؤثر بر گزینش‌پذیری و کارایی فرآیندهای فلوتاسیون و به ویژه، بازیابی ذرات ریز است. با توجه به اینکه فلوتاسیون یک فرآیند پیوسته و وابسته به زمان است، در این پژوهش تأثیر پارامترهای عملیاتی در بازه‌های زمانی متوالی بر نرخ دنباله‌روی مواد خاکستر در فلوتاسیون یک نمونه زغال سنگ مورد بررسی قرار گرفت. تأثیر پارامترهای مورد نظر شامل درصد جامد، غلظت کلکتور و کفساز، سرعت همزن و اندازه ذرات بر ضریب دنباله‌روی و بازیابی آب در زمان‌های مختلف با استفاده از یک طرح آزمایشی پاسخ سطح D-optimal ارزیابی شد. مطالعات نشان داد که برخی از پارامترها، به ویژه اندازه ذرات و دانسیته پالپ، با گذشت زمان می‌توانند تأثیراتی کاملاً متفاوت از آنچه تاکنون در مراجع ارائه شده است از خود نشان دهند. چنانچه نتایج آزمایشگاهی تأیید کرد، رفتارهای غیرمعمول مشاهده شده را می‌توان به مکانیزم‌های دنباله‌روی متفاوت نسبت داد. همچنین، مشاهده شد که مکانیزم دنباله‌روی غالب در سیستم با زمان تغییر می‌کند. به علاوه، تحلیل‌های آماری طرح آزمایشی نشان داد که تأثیر برخی پارامترها با گذشت زمان، از ابتدا تا انتهای فرآیند فلوتاسیون تغییر می‌کند. نتایج نشان داد اندازه ذرات و دانسیته پالپ مؤثرترین پارامترها بر نرخ دنباله‌روی و بازیابی آب هستند. کمترین تأثیر متعلق به غلظت کلکتور و کفساز بود. تأثیر متقابل میان درصد جامد و اندازه ذرات نیز تنها تأثیر متقابل مؤثر تشخیص داده شد.

**کلمات کلیدی:** فلوتاسیون زغال سنگ، پارامترهای عملیاتی، توالی زمانی، ضریب دنباله‌روی، بازیابی آب.

---